

$E1$ and $E2$ strength in ^{24}Mg and ^{26}Mg observed in α -capture reactions*

E. Kuhlmann,^{†‡} E. Ventura,[§] J. R. Calarco, D. G. Mavis, and S. S. Hanna
Department of Physics, Stanford University, Stanford, California 94305

(Received 23 December 1974)

Excitation functions and angular distributions of the reactions $^{20,22}\text{Ne}(\alpha, \gamma_0)$ were used to study the distribution of $E2$ strength in the energy regions 14–22 MeV of $^{24,26}\text{Mg}$, as well as to probe the importance of isospin in the decay of the $E1$ giant resonance in these nuclei. It was found that the $E2$ strength in the (γ, α_0) channel is rather uniformly distributed and accounts for about 10% of the energy weighted sum rule in each nucleus. Together with the $E2$ strength observed in lower resonances, about 45% of the sum rule is accounted for. No evidence for a compact $E2$ resonance is found. A comparison of the $E1$ distribution and total strength in the (γ, α_0) channel of the giant dipole resonances in $^{24,26}\text{Mg}$ indicates that isospin conservation may be important in these reactions. Information was also obtained on the reactions $^{20,22}\text{Ne}(\alpha, \gamma_1)$.

NUCLEAR REACTIONS $^{20}\text{Ne}(\alpha, \gamma)$, $E = 2.5\text{--}20$ MeV; $^{22}\text{Ne}(\alpha, \gamma)$, $E = 4.5\text{--}16$ MeV; measured $\sigma(E, E_\gamma, \theta_\gamma)$. $^{24,26}\text{Mg}$ deduced $E1$, $E2$ strength. Enriched targets.

I. INTRODUCTION

Recently, in a variety of inelastic scattering experiments of high energy electrons^{1,2} and nuclear particles,^{3–5} a resonance has been observed which is interpreted as an isoscalar $E2$ (or $E0$) giant resonance. This $E2$ (or $E0$) resonance is reported to lie about 3 MeV below the well-known giant dipole resonance (GDR) or at an approximate energy of $63A^{-1/3}$ MeV, to have a width of about 4 MeV, to exhaust (if $E2$ in nature) the isoscalar $E2$ sum rule, and to be a universal characteristic of all nuclei. To shed more light on the nature and multipolarity of this new resonance, we have studied it by radiative capture reactions, which have been used extensively for many years to study giant resonances. Although the major strength observed in these reactions is electric dipole in character, the $E2$ strength shows up strongly in interference with the dominant $E1$ radiation.

Some of the best evidence from capture reactions which bears directly on the giant quadrupole resonance (GQR) comes from (α, γ_0) measurements.^{6–8} These data show an appreciable amount of isoscalar $E2$ strength (10–20% of the sum rule) and have been interpreted as being consistent with the existence of a GQR.⁹ In this paper we report a search for isoscalar $E2$ strength in the light nuclei ^{24}Mg and ^{26}Mg with the reactions $^{20}\text{Ne}(\alpha, \gamma)\text{-}^{24}\text{Mg}$ and $^{22}\text{Ne}(\alpha, \gamma)\text{-}^{26}\text{Mg}$. The observations covered the energy range from the Coulomb barrier up into the region of the GDR, spanning the region of the reported $E2$ resonance.

The (α, γ_0) reaction on even-even nuclei provides a sensitive means of measuring $E2$ strength since

the angular distribution is uniquely determined by the multipolarity of the radiation. Furthermore, for a self-conjugate nucleus like ^{24}Mg the $E1$ radiation may be suppressed since only $T=0$ resonances can be formed directly in α capture and these are forbidden by isospin to decay by $E1$ radiation. Hence the $E1$ radiation must occur by isospin mixing. There is evidence in these reactions that the isospin mixing may be large.⁶ Nevertheless, it turns out that the dipole radiation is weak in both the conjugate and the nonconjugate nuclei so that very small amounts of $E2$ radiation can be detected in the (α, γ_0) reaction.

A second objective of these studies was to measure the amount of $E1$ radiation in order to study the question of the isospin mixing mentioned above, as well as to probe the importance of the α decay of the GDR. Since the isospin selection rule on $E1$ decay does not apply for a nonconjugate nucleus such as ^{26}Mg , a comparison of the (α, γ) reaction for ^{24}Mg and ^{26}Mg should give valuable information on the α width of the GDR.

The reactions $^{20}\text{Ne}(\alpha, \gamma_1)\text{-}^{24}\text{Mg}$ and $^{22}\text{Ne}(\alpha, \gamma_1)\text{-}^{26}\text{Mg}$ were also studied in some detail. Yield curves as well as angular distributions were measured, although the analysis of the angular distributions is not as straightforward as in the case of the (α, γ_0) reactions.

II. EXPERIMENTAL PROCEDURE AND ANALYSIS

α particle beams from the Stanford FN tandem Van de Graaff accelerator were used to bombard a target of either ^{20}Ne gas (99.95%) or ^{22}Ne gas (97.0%) contained in a cylindrical gas cell. The

cell, 1.9 cm in diameter, was filled to a pressure of about $\frac{1}{4}$ atmosphere, which corresponds to a target thickness of 400 keV at 8 MeV bombarding energy. The beam entered the cell through a Ni foil 0.125×10^{-3} cm thick (corresponding to an energy loss of 400 keV at 8 MeV) and was stopped within the cell on a thick Au backing. The capture γ rays were detected in the Stanford NaI spectrometer¹⁰ placed at a distance of 63 cm from the target spot. The lead collimator of the detector subtended a half-angle of 7° or a solid angle of 0.045 sr. A typical spectrum obtained with this geometry for the reaction $^{20}\text{Ne}(\alpha, \gamma)^{24}\text{Mg}$ is shown in Fig. 1. The ground state transition γ_0 and the excited state transition γ_1 are easily resolved in this spectrum. To obtain the yields of γ_0 and γ_1 a computer program¹¹ was employed which fits standard line shapes to the experimental spectrum by a means of a least-squares fitting routine. The solid line in Fig. 1 shows the final fit with the dashed curves giving the individual fits to γ_0 and γ_1 . The total efficiency of the NaI assembly as defined in Ref. 10 was about 70% and varied by less than 10% over the energy range covered in this experiment. The final data have been corrected for this variation.

Excitation functions at $\theta_\gamma = 130^\circ$ and angular distributions were measured with the setup described above. For the angular distributions, generally five angles equally spaced from 45 to 135° were measured sequentially, and the sequence was repeated at least once. In some cases spectra were obtained also at 0 and 15° . Each angular distribution for γ_0 and γ_1 can be fitted by an expansion of

Legendre polynomials

$$W(\theta) = \sum_{k=0}^4 A_k P_k(\cos\theta) = A_0 \left[1 + \sum_{k=1}^4 a_k P_k(\cos\theta) \right], \quad (1)$$

since only dipole and quadrupole radiations are significant. However, it turns out that for γ_0 for zero-spin nuclei only three of the five expansion coefficients A_k are independent. Because the initial channel-spin is zero, only states with natural parity can be excited, i.e., $1^-, 2^+, \dots$, formed by pure p, d, \dots wave capture, respectively, and decays to the 0^+ ground state involve only $E1$ and $E2$ radiation. Then

$$\sum_{k=\text{even}} A_k = \sum_{k=\text{odd}} A_k = 0. \quad (2)$$

With these restrictions the γ_0 angular distributions can be fitted by the expression

$$W(\theta) = \frac{1}{4\pi} [(\sigma_{E1} + \sigma_{E2}) - (\sigma_{E1} - 0.71\sigma_{E2})P_2 - 1.71\sigma_{E2}P_4 - 2.68(\sigma_{E1}\sigma_{E2})^{1/2} \cos\delta(P_1 - P_3)]. \quad (3)$$

The cross sections σ_{E1} and σ_{E2} denote the partial cross sections for capture through 1^- and 2^+ resonances, respectively, and δ is the phase difference of the corresponding p and d waves. It follows from this simple expression that the (α, γ_0) capture reaction is ideally suited for extracting quantitatively the amount of $E2$ strength underlying the dominant $E1$ yield.

No such restrictions hold for the angular distributions of γ_1 leading to the first excited state with $J^\pi = 2^+$. In this case $E1, M1,$ and $E2$ decay can be expected from states with $J^\pi = (1^-, 3^-), 2^+$, and $(0^+, 2^+, 4^+)$, respectively, and $W(\theta)$ will be much more complicated. Since a detailed analysis including interference among all states and multiplicities is not possible for the γ_1 angular distributions, only fits in terms of Legendre polynomials will be given. Since in general the angular distributions were measured at five angles only, the expansion was carried out only up to P_3 to provide at least one degree of freedom in the fitting procedure. Moreover, it was found that fits to the γ_1 distributions including only terms up to P_2 were satisfactory; in general no significant improvement was gained in expanding the fits up to P_3 , and the a_3 coefficients thus obtained were close to zero, as will be seen later. In the analysis of the angular distributions of γ_0 and γ_1 the effect of the solid angle of the detector, the correction for the Doppler shift of the radiation, and small asymmetries arising from target location were all taken

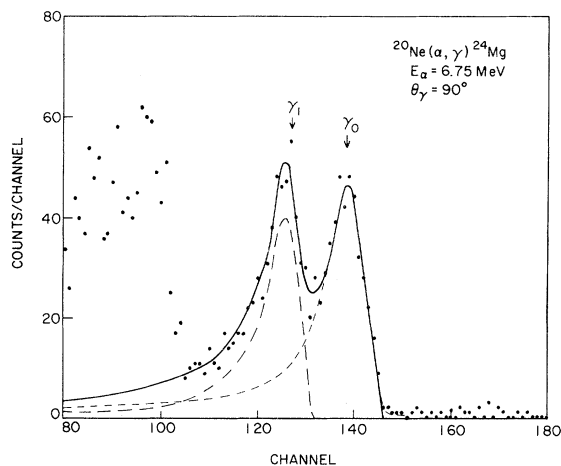


FIG. 1. A typical spectrum for the reaction $^{20}\text{Ne}(\alpha, \gamma)^{24}\text{Mg}$ taken for 600 μC . The solid line shows a least-squares fit to the spectrum the two components of which are indicated by the dashed lines.

into account.

In order to assess the E_1 and isoscalar E_2 strengths observed in this experiment we employed the sum rules¹²

$$\begin{aligned}\sigma_0(E1) &= \int \sigma(E1)dE \\ &= 60 NZ/A \text{ MeV mb},\end{aligned}\quad (4)$$

$$\begin{aligned}\sigma_{-2}(E2) &= \int \sigma(E2)/E_x^2 dE \\ &= 0.25Z^2A^{-1}\langle R^2 \rangle \\ &= 0.22Z^2A^{-1/3} \mu\text{b/MeV},\end{aligned}\quad (5)$$

with $\langle R^2 \rangle = \frac{3}{5}r_0^2A^{2/3}$ and $r_0 = 1.2$ fm.

III. RESULTS

A. The reaction $^{20}\text{Ne}(\alpha, \gamma)^{24}\text{Mg}$

The upper part of Fig. 2 shows the yield curve obtained at $\theta_\gamma = 130^\circ$ over an α -energy range which corresponds to excitation energies in ^{24}Mg extending from $E_x = 11.5$ to 22.5 MeV. The average step size was 150 keV. The α -energy scale has been

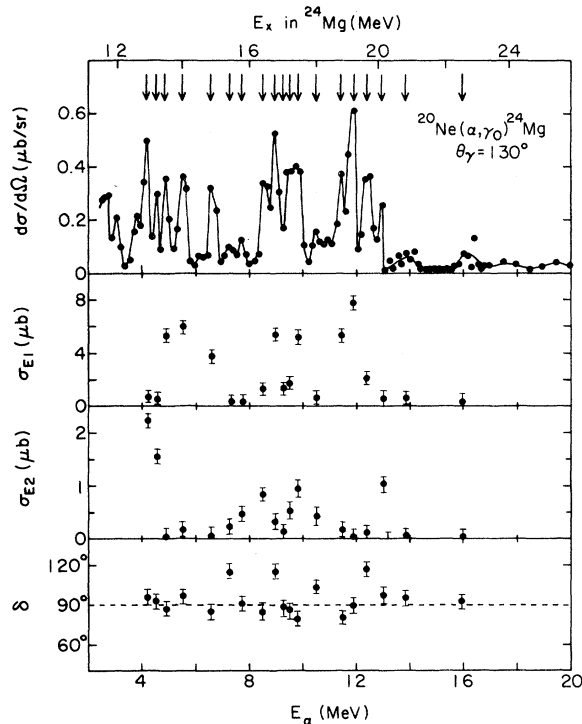


FIG. 2. Top: excitation function at $\theta = 130^\circ$ for the reaction $^{20}\text{Ne}(\alpha, \gamma)^{24}\text{Mg}$. The arrows indicate energies at which angular distributions were studied. Middle: the extracted E_1 and E_2 total cross sections for the (α, γ_0) reaction. Bottom: the E_2 phase δ , relative to the E_1 phase, which is arbitrarily set to zero.

corrected for the energy loss in the Ni entrance foil (300–700 keV) and has been adjusted for one-half the target thickness (75–180 keV). The 130° angle of observation was chosen so as to favor E_2 radiation (which is a maximum at 135°) while at the same time not suppressing greatly E_1 radiation (which is reduced to about 60% at 130°). Three different regions can be seen: (1) between 12 and 15 MeV excitation energy there are many narrow and isolated peaks which correspond to individual resonances which are partly known from previous (α, γ_0) studies,¹³ (2) between 15 and 21 MeV broader structures appear, and (3) above 21 MeV the (α, γ_0) cross section becomes very small, at least partly as the result of the opening of various other decay channels. The absolute cross sections averaged over energy intervals are given in Table I.

The arrows in Fig. 2 indicate key energies at which angular distributions were measured. A representative set is shown in Fig. 3. The angular distributions were analyzed by means of Eq. (3) with the extracted quantities σ_{E1} , σ_{E2} , and δ shown in the lower part of Fig. 2. The results in the energy range up to $E_x = 14.3$ MeV are in excellent agreement with the work of Highland and Thwaites,¹³ who studied the $^{20}\text{Ne}(\alpha, \gamma_0)^{24}\text{Mg}$ reaction with rather thin implanted ^{20}Ne targets (≤ 50 keV at $E_\alpha = 5$ MeV), although their detector could not resolve γ_0 and γ_1 . They report resonances at $E_\alpha = 4.193$, 4.528, and 5.653 MeV, and a barely resolved doublet at 4.92 MeV with assignments of 2^+ , 2^+ , 1^- , and $(1^-, 2^+)$, respectively. These can be identified with the four isolated peaks at 4.18, 4.51, 5.64, and 4.85 MeV studied in the present experiment by angular distributions. A 1^- assignment can also be given to the resonance observed at $E_\alpha = 6.60$ MeV corresponding to a state at 14.8 MeV.

In the energy range above $E_x = 15$ MeV the con-

TABLE I. The averaged absolute cross sections $\bar{\sigma}(\alpha, \gamma_0)$ and $\bar{\sigma}(\alpha, \gamma_1)$ for the reactions $^{20}\text{Ne}(\alpha, \gamma)^{24}\text{Mg}$ and $^{22}\text{Ne}(\alpha, \gamma)^{26}\text{Mg}$.

ΔE_x (MeV)	$^{20}\text{Ne}(\alpha, \gamma)^{24}\text{Mg}$		$^{22}\text{Ne}(\alpha, \gamma)^{26}\text{Mg}$	
	$\bar{\sigma}(\alpha, \gamma_0)^a$ (μb)	$\bar{\sigma}(\alpha, \gamma_1)^b$ (μb)	$\bar{\sigma}(\alpha, \gamma_0)^a$ (μb)	$\bar{\sigma}(\alpha, \gamma_1)^b$ (μb)
11.4–14.4	3.2	3.9
14.4–17.8	3.1	4.8	9.2	8.6
17.8–20.2	3.6	9.6	3.0	4.5
20.2–23.8	0.6	1.8	0.9	2.8
23.8–26.0	0.4	0.6

^a Angular distribution assumed to be of the form $W(\theta) = \sin^2\theta$.

^b Angular distribution assumed to be isotropic.

tribution from the dominant $E1$ decay is on the average only a factor of 4 stronger than the $E2$ decay. This might indicate a strong inhibition of $E1$ strength due to isospin and will be discussed in more detail in Sec. IV B in comparison with the results from $^{22}\text{Ne}(\alpha, \gamma_0)^{26}\text{Mg}$. However, the fact that the excitation function shows strong fluctuations with the α energy and does not exhibit a giant resonance shape suggests that the α -capture reaction goes mostly via long-lived compound nuclear configurations in which appreciable isospin mixing occurs.

It can be seen in Fig. 2 that there is no concentration of $E2$ strength which would correspond to a narrow GQR at $63A^{-1/3} = 22$ MeV. Also, the relative phase δ does not show a drastic resonant effect in this region, but remains rather close to 90° . This appears to be a general feature of α -capture reactions at high excitation energies^{6,7} and can be explained by assuming that the overlapping 1^- and 2^+ levels interfere in such a way that in the interference term of the measured angular distributions the various separate terms with both positive and negative signs cancel each other on the average.

If the α -capture data are converted into the (γ, α_0) process by detailed balance, the yield curve can be compared with other photonuclear reactions such as $^{24}\text{Mg}(\gamma, p_0)^{23}\text{Na}$,¹⁴ as is shown in Fig. 4. The $^{24}\text{Mg}(\gamma, p_0)^{23}\text{Na}$ yield curve [Fig. 4(c)]

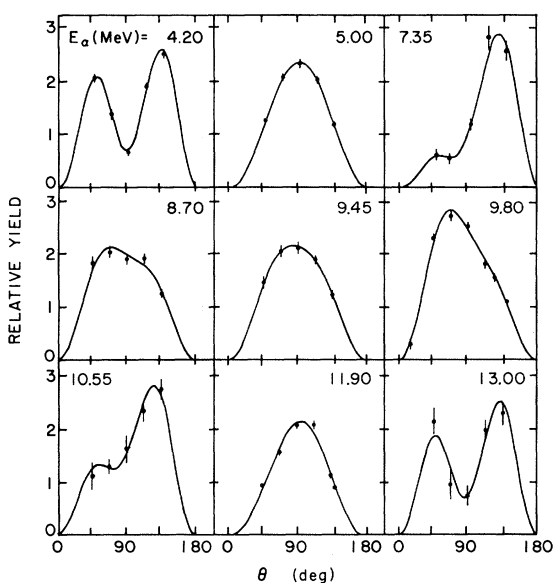


FIG. 3. Typical angular distributions for the reaction $^{20}\text{Ne}(\alpha, \gamma_0)^{24}\text{Mg}$. Note the almost pure $E1$ character of the distributions at $E_\alpha = 5.00$ and 11.90 MeV in marked contrast to the predominantly $E2$ character at 4.20 and 13.00 MeV. The solid lines are fits in terms of Eq. (3).

also shows an appreciable amount of fine structure and it has been reported¹⁴ that this reaction proceeds to a large extent through a compound nuclear configuration. The fact that no significant cross correlation is observed between the (γ, α_0) and the (γ, p_0) channels (see Sec. III E) is in nice agreement with the assumption that the fine structure is in fact due to fluctuations arising from the presence of many strongly overlapping levels in the compound nucleus.

Figure 4(a) displays the distribution of $E2$ strength observed in the $^{24}\text{Mg}(\gamma, \alpha_0)^{20}\text{Ne}$ reaction. The integrated $E2$ strength in the energy range 12.0 – 22.5 MeV is about 12% of the energy weighted sum rule Eq. (5) (see Table II). In the same energy region the $E1$ strength is found to be only 0.33% of the corresponding sum rule Eq. (4) (see Table III). This result will be discussed in more detail in Sec. IV B.

B. The reaction $^{20}\text{Ne}(\alpha, \gamma_1)^{24}\text{Mg}$

The top part of Fig. 5 shows the yield curve at $\theta_\gamma = 130^\circ$ for γ_1 leading to the first excited state in

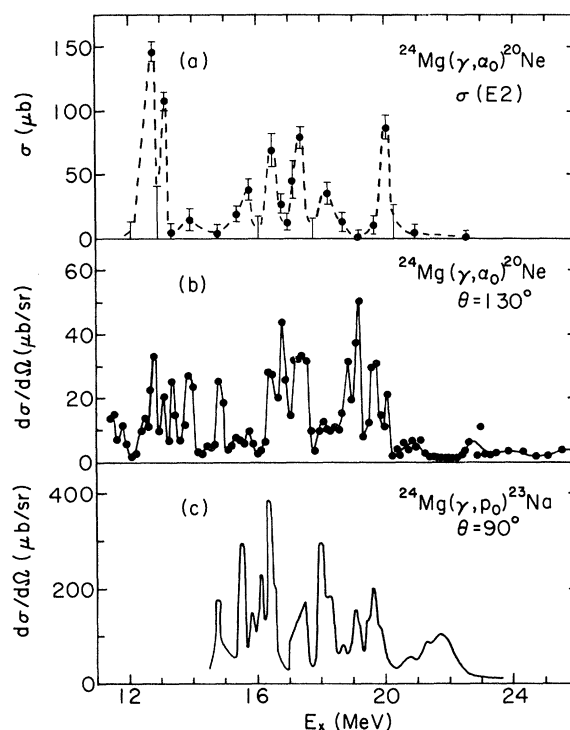


FIG. 4. (a) the extracted total $E2$ cross section converted by detailed balance to that for the reaction $^{24}\text{Mg}(\gamma, \alpha_0)^{20}\text{Ne}$. (b) the 130° excitation function ($E1 + E2$) for $^{24}\text{Mg}(\gamma, \alpha_0)^{20}\text{Ne}$. (c) the excitation function at $\theta = 90^\circ$ for $^{24}\text{Mg}(\gamma, p_0)^{23}\text{Na}$ obtained by detailed balance from $^{23}\text{Na}(p, \gamma)^{24}\text{Mg}$ (Ref. 14).

TABLE II. Summary of $E2$ strengths in $^{24,26}\text{Mg}(\gamma, \alpha_0)$ (see text) given in percent of the $E2$ sum rule [Eq. (5)].

Nucleus	ΔE (MeV)	$\int \sigma(E2)/E^2 dE$ (%)	ΔE (MeV)	$\int \sigma_{\text{tot}}^{\text{CN}}(E2)/E^2 dE$ (%)
^{24}Mg	12.0–22.5	11.8 ± 1.0	0–22.5	120 ± 30
^{26}Mg	15.0–21.4	6.0 ± 2.0	0–21.4	290 ± 80

^{24}Mg at 1.37 MeV. The α -energy scale has been corrected for the energy loss in the entrance foil and adjusted for the target thickness as described in Sec. III A. The average cross section is generally higher than that observed for the ground state decay (Table I). The yield curve for γ_1 also shows a great deal of structure with a somewhat greater concentration of strength in the region $E_x = 16.5$ to 20 MeV than observed for γ_0 . Above $E_x = 21$ MeV the yield becomes very small.

The expansion coefficients obtained in fitting the γ_1 angular distributions to a sum over Legendre polynomials are shown in the lower part of Fig. 5. It is interesting to note the almost smooth variation in the coefficient a_2 which at the lower bombarding energies has an average value of $a_2 = +0.5$, crosses zero at the medium energies, and reaches an average value of $a_2 = -0.5$ at the higher bombarding energies. A value of $a_2 = -0.40$ is expected for $E1$ decay originating from 3^- levels, which might indicate that with increasing energy the $^{20}\text{Ne}(\alpha, \gamma_1)$ reaction proceeds to a large extent through 3^- levels. But, as was mentioned earlier, the complexity of the γ_1 decay makes it impossible to include all possible interference effects in the analysis of the angular distributions.

C. The reaction $^{22}\text{Ne}(\alpha, \gamma_0)^{26}\text{Mg}$

The reaction $^{22}\text{Ne}(\alpha, \gamma_0)^{26}\text{Mg}$ ($Q = 10.61$ MeV) was investigated over the energy range of $E_\alpha = 5$ to 16 MeV corresponding to excitation energies in ^{26}Mg from 14.6 to 24.0 MeV. The γ_0 yield observed at $\theta_\gamma = 130^\circ$ is shown at the top of Fig. 6. Up to α en-

ergies of 11 MeV the measurements were taken in steps of 150 keV, and thereafter in steps of 200 keV. It is seen that most of the yield is concentrated in a region between $E_x = 15$ and 18.5 MeV where the average cross section is about a factor of 3 higher than the cross section for α capture by the self-conjugate nucleus ^{20}Ne (see Table I). Above $E_x = 18.5$ MeV the cross section becomes very small and of comparable size to the $^{20}\text{Ne}(\alpha, \gamma)$ reaction. This result might be attributed to the fact that this is the region of the T_2 giant $E1$ resonance which is isospin forbidden in both reactions $^{20}\text{Ne}(\alpha, \gamma)$ and $^{22}\text{Ne}(\alpha, \gamma)$, see Sec. IV B.

Angular distributions were measured on top of the main peaks of the yield curve as indicated by the arrows in Fig. 6, and analyzed as described in Sec. II. The results are shown in the lower part of Fig. 6. In the region of the main yield the observed radiation is about 95% $E1$ in character. The underlying $E2$ strength found in this region is of about the same magnitude as that in the same region in ^{24}Mg (see Table II) with an average cross section of about $0.8 \mu\text{b}$. By means of the principle of detailed balance, the $E2$ cross sections and the total yield curve were inverted to the (γ, α_0) process, as shown in Figs. 7(a) and 7(b), respectively, and compared with the photoneutron cross section data¹⁵ in Fig. 7(c). The amount of $E2$ strength determined in this experiment in the energy range $E_x = 15.0$ to 21.4 MeV is about $6 \pm 2\%$ of the sum rule [Eq. (5)]. In the integration of the $E2$ strength it was assumed that the yield in the valleys of the excitation curve consists of pure $E2$ radiation only. The error originating from this assumption is

TABLE III. A comparison of the integrated $E1$ strengths found in various reactions in the GDR's of ^{24}Mg and ^{26}Mg . The strengths are given in percent of the $E1$ sum rule [Eq. (4)].

Nucleus	(γ, α)		$(\gamma, p_0)^a$		$(\gamma, n)^b$		$(e, e')^c$	
	ΔE (MeV)	$\int \sigma(E1)dE$ (%)	ΔE (MeV)	$\int \sigma(E1)dE$ (%)	ΔE (MeV)	$\int \sigma(E1)dE$ (%)	ΔE (MeV)	$\int \sigma(E1)dE$ (%)
^{24}Mg	14.6–20.6	0.33	15.5–23.0	3.3	16.5–28.0	14.0	16.0–22.0	30.0
^{26}Mg	14.8–21.0	0.70	11.0–28.0	58.0	14.5–28.0	48.0

^a Reference 14.^b Reference 15.^c References 19 and 27.

small and is included in the quoted error of the total strength.

As can be seen in Fig. 6, the observed strength in $^{26}\text{Mg}(\gamma, \alpha_0)$ is almost pure $E1$. Thus, the $E1$ strength in the α_0 decay channel was determined by simply integrating along the solid curve in Fig. 7(b) and was found to be 0.7% of the sum rule Eq. (4), as will be discussed in Sec. IV B.

D. The reaction $^{22}\text{Ne}(\alpha, \gamma_1)^{26}\text{Mg}$

The yield of the γ rays leading to the first excited state in ^{26}Mg at 1.81 MeV is shown in the upper part of Fig. 8. Two strong peaks at $E_\alpha = 6.5$ and 12.3 MeV are observed superimposed on a fluctuating yield with an average cross section of $0.4 \mu\text{b}/\text{sr}$. Above $E_x = 22$ MeV the cross section becomes very small, as was found for $^{20}\text{Ne}(\alpha, \gamma_1)$. The average cross section for $^{22}\text{Ne}(\alpha, \gamma_1)$ is found to be of the same order of magnitude as those of the other reactions (see Table I). The structure observed in the yield curve for γ_1 is correlated to some extent with that of γ_0 as will be discussed in Sec. III E. No such correlation was observed in the case of ^{20}Ne .

The results of the angular distribution measure-

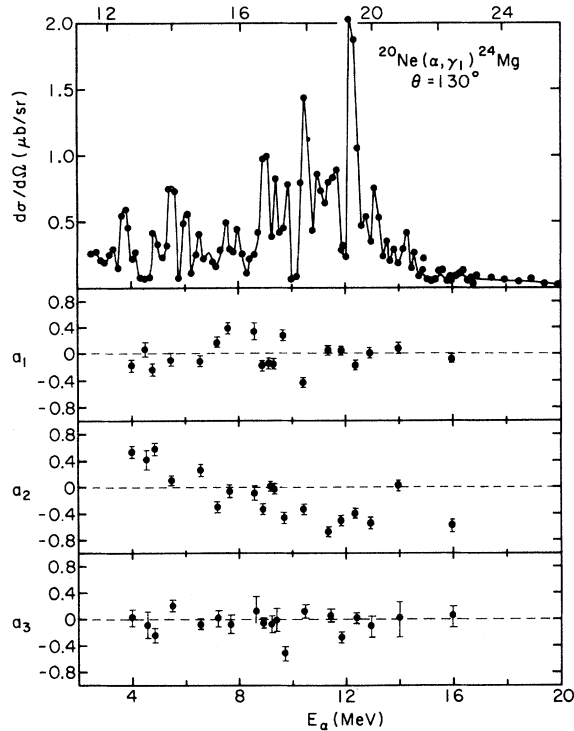


FIG. 5. The excitation function at $\theta = 130^\circ$ and the coefficients a_1 , a_2 , and a_3 from a Legendre polynomial fit to the angular distributions of the reaction $^{20}\text{Ne}(\alpha, \gamma_1)^{24}\text{Mg}^*$ (1.37 MeV). Note the systematic change of a_2 from $+0.5$ at $E_\alpha = 4$ MeV to -0.5 at 16 MeV.

ments are shown in the lower part of Fig. 8. The expansion coefficients a_k are rather uniformly distributed around average values of $a_1 = +0.01$, $a_2 = -0.12$, and $a_3 = +0.03 (\pm 0.06)$, reflecting the almost constant shape of the γ_1 angular distributions. This is in marked contrast to the results found for the γ_1 angular distributions in the α capture by ^{20}Ne , where the a_2 coefficient was found to change from large positive to large negative values with increasing energy (see Sec. III B). It is interesting to note that the average value obtained for a_2 is close to the predicted value of $a_2 = -0.10$ for $E1$ decay through 1^- levels.

E. Structure in the yield curves

The excitation functions for α capture into the giant resonance regions of ^{24}Mg and ^{26}Mg do not exhibit the giant resonance shapes observed in proton capture reactions. Instead, they show a large amount of structure spread over a wide re-

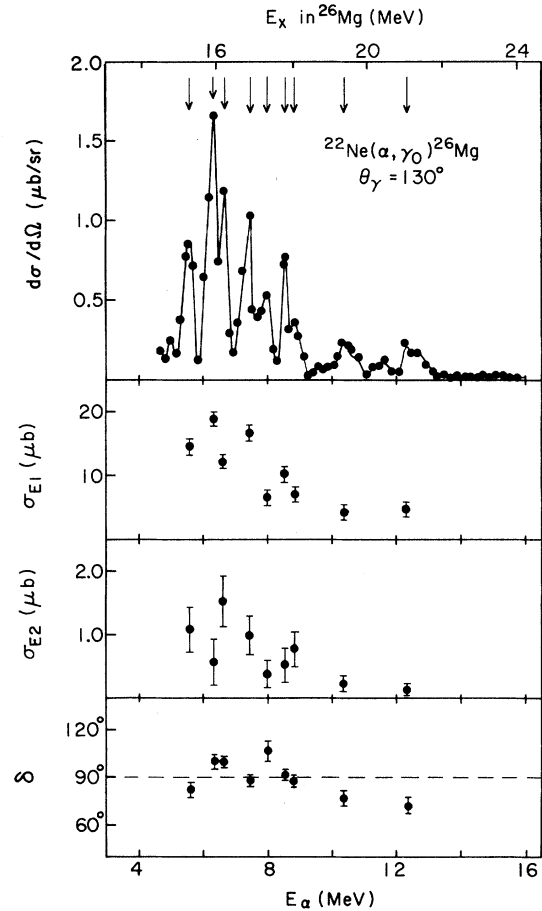


FIG. 6. Top: excitation function for the reaction $^{22}\text{Ne}(\alpha, \gamma_0)^{26}\text{Mg}$ at $\theta = 130^\circ$. Middle: the extracted $E1$ and $E2$ total cross sections for the (α, γ_0) reaction. Bottom: the $E2$ phase relative to the $E1$ phase.

gion below the GDR which seems to be a common feature of α capture reactions.⁶⁻⁸ A detailed analysis of the fine structure in the $^{24}\text{Mg}(\alpha, \gamma_0)^{28}\text{Si}$ reaction has been given⁶ in terms of Ericson fluctuations,¹⁶ and it was shown that the reaction proceeds about 80% of the time through a compound nucleus.

Since the yield curves in the present experiment were obtained with rather thick targets and with step sizes of $\Delta E \geq 150$ keV, a large amount of fine structure, if present, would not have been observed. Hence an autocorrelation analysis of the yield curves is not very meaningful. However, some information may be obtained by comparing the structure observed in the γ_0 and the γ_1 yield curves for both reactions $^{20}\text{Ne}(\alpha, \gamma)$ and $^{22}\text{Ne}(\alpha, \gamma)$. Additionally, a cross-correlation study was performed on the reactions $^{23}\text{Na}(p, \gamma)^{24}\text{Mg}$ ¹⁴ and $^{20}\text{Ne}(\alpha, \gamma)^{24}\text{Mg}$.

The cross-correlation functions were calculated

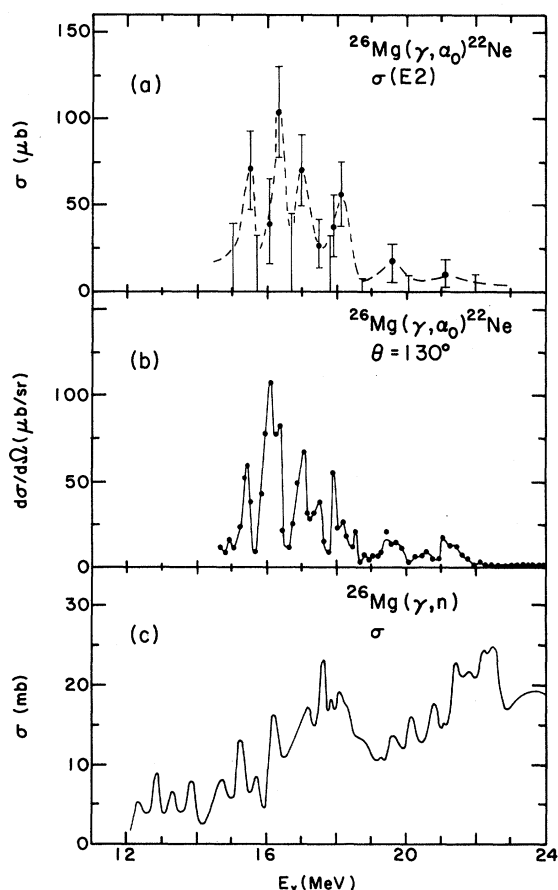


FIG. 7. (a) the extracted $E2$ cross section converted by detailed balance to the total $E2$ cross section for the reaction $^{26}\text{Mg}(\gamma, \alpha_0)^{22}\text{Ne}$. (b) the excitation function ($E1 + E2$) at $\theta = 130^\circ$ for the reaction $^{26}\text{Mg}(\gamma, \alpha_0)^{22}\text{Ne}$. (c) the cross section for $^{26}\text{Mg}(\gamma, n)$ obtained with monoenergetic photons (Ref. 15).

as outlined in Ref. 6. Briefly, we used the basic cross-correlation function

$$R(\epsilon) = \frac{\Delta E}{E_2 - E_1} \sum_{E=E_1}^{E_2} \left[\frac{\sigma_1(E)}{\sigma_1(E)} - 1 \right] \left[\frac{\sigma_2(E+\epsilon)}{\sigma_2(E+\epsilon)} - 1 \right], \quad (6)$$

where σ_1 and σ_2 denote the cross sections of the two reactions to be compared within the energy range $(E_2 - E_1)$. The variable ϵ is defined by $\epsilon = n\Delta E$, where n is an integer and ΔE the average step size. Since the fluctuations observed in the yield curves are superimposed on a broader structure, the averaging interval $2\delta E$ used to obtain the average cross sections $\overline{\sigma_1(E)}$ and $\overline{\sigma_2(E+\epsilon)}$ is of some importance. As in Ref. 6, we assumed

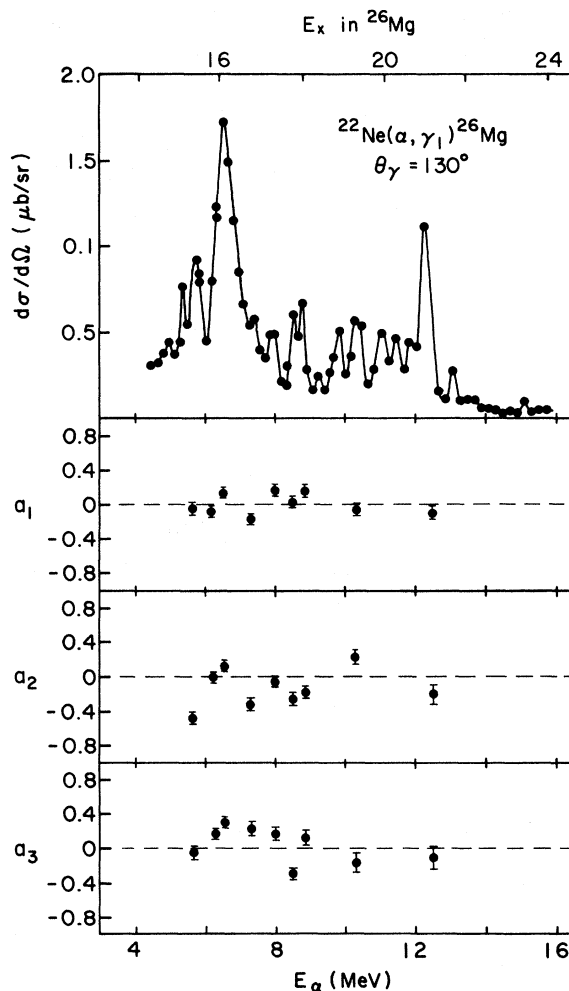


FIG. 8. The excitation function at $\theta = 130^\circ$ and the coefficients a_1 , a_2 , and a_3 from a Legendre polynomial fit to the angular distributions for the reaction $^{22}\text{Ne}(\alpha, \gamma_1)^{26}\text{Mg}^*$ (1.81 MeV). In this case the a_2 fluctuates about a value of -0.12 in contrast to the behavior for $^{20}\text{Ne}(\alpha, \gamma_1)$.

as a first step that no gross structure is present which allowed us to make the averaging interval $2\delta E$ equal to $(E_2 - E_1)$, yielding a cross correlation function C_1 . To reduce the influence of the gross structure we then subtracted from C_1 a cross correlation function C_2 which differed from C_1 in that in the numerator the cross sections $\sigma_1(E)$ and $\sigma_2(E + \epsilon)$ were replaced by $\langle \sigma_1(E) \rangle$ and $\langle \sigma_2(E + \epsilon) \rangle$, respectively, where the averages were taken over a 2 MeV wide interval $(E - 1) \text{ MeV} \leq E \leq (E + 1) \text{ MeV}$.

The cross-correlation functions $C(\epsilon) = C_1(\epsilon) - C_2(\epsilon)$ thus obtained for the reactions $^{20}\text{Ne}(\alpha, \gamma_0)$ and $^{20}\text{Ne}(\alpha, \gamma_1)$, the reactions $^{20}\text{Ne}(\alpha, \gamma_0)$ and $^{23}\text{Na}(p, \gamma_0)$, and the reactions $^{22}\text{Ne}(\alpha, \gamma_0)$ and $^{22}\text{Ne}(\alpha, \gamma_1)$ are shown in Figs. 9(a), b, and c, respectively, for positive and negative ϵ . The finite range of energies over which the excitation functions were measured causes oscillations around $C(\epsilon) = 0$. According to Ref. 17 the amplitude of these oscillations can be estimated to be of the order

$$c_{\text{osc}} = (\pi/2nN_1N_2)^{1/2}, \quad (7)$$

where n is the number of independent data points ($n = 50$ in the present experiment) and N_1 and N_2 are the effective number of uncorrelated equal channels through which the two reactions proceed. The quantities N_1 and N_2 can be estimated to be of the order of unity for the ground state transitions

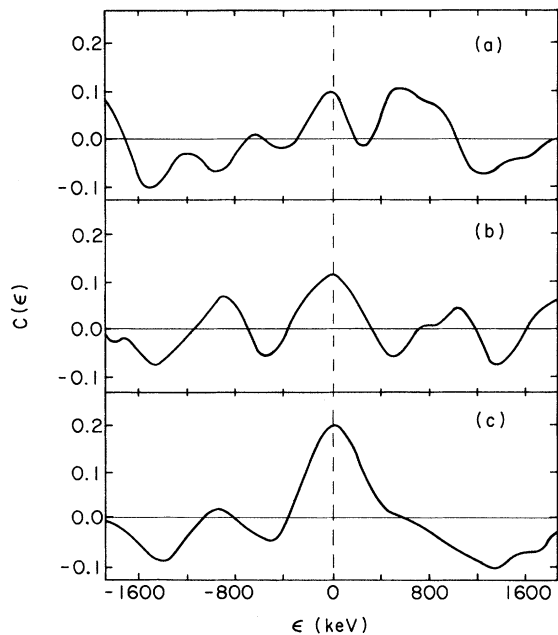


FIG. 9. Cross-correlation functions $C(\epsilon)$ for (a) $^{20}\text{Ne}(\alpha, \gamma_0)$ and $^{20}\text{Ne}(\alpha, \gamma_1)$, (b) $^{24}\text{Mg}(\gamma, \alpha_0)$ and $^{24}\text{Mg}(\gamma, p_0)$ (Ref. 14), and (c) $^{22}\text{Ne}(\alpha, \gamma_0)$ and $^{22}\text{Ne}(\alpha, \gamma_1)$. A significant correlation exists only in the last case.

γ_0 , but they are definitely greater than unity for the γ_1 transitions. Thus we obtain oscillation amplitudes of the order of <0.17 , ≈ 0.17 , and <0.17 for the reactions compared in Figs. 9(a), (b), and (c), respectively. When the cross-correlation functions in Fig. 9 are compared with these estimates, it is apparent that the correlations are not significantly different from zero for those reactions that form ^{24}Mg as a final nucleus [Figs. 9(a) and (b)], whereas there is a significant correlation between the reactions $^{22}\text{Ne}(\alpha, \gamma_0)$ and $^{22}\text{Ne}(\alpha, \gamma_1)$ [Fig. 9(c)]. For pure fluctuations, a null result is expected in the cross-correlation between two reactions. Thus, the zero value found for the $^{20}\text{Ne}(\alpha, \gamma_0\gamma_1)$ reactions indicates that the reaction proceeds predominantly through compound nuclear channels. On the other hand, the nonzero value observed for the cross-correlation of the $^{22}\text{Ne}(\alpha, \gamma_0\gamma_1)$ reactions, together with the fact that the angular distributions for γ_0 and γ_1 exhibit an almost constant shape with an a_2 coefficient close to that expected for decay from 1^- levels, indicates that the $^{22}\text{Ne}(\alpha, \gamma_0\gamma_1)$ reactions might proceed mainly through isolated 1^- levels. This is not unexpected since the $E1$ decay of 1^- levels in ^{26}Mg is isospin allowed, whereas it is forbidden in ^{24}Mg .

IV. DISCUSSION

A. Excitation of the giant quadrupole resonance

According to the hydrodynamic model¹⁸ the giant quadrupole resonance should lie at an energy of about $63A^{-1/3} \text{ MeV}$. For ^{24}Mg this turns out to be at 22 MeV, which is almost the center of the giant dipole resonance as observed, for example, in electron scattering.¹⁹ From a comparison of the respective sum rules for excitation of the GQR, Eq. (5), and the GDR, Eq. (4), one finds

$$\frac{E_{\text{GQR}}^2 \sigma_{-2}(E2)}{\sigma_0(E1)} \approx 1\%.$$

Thus, the question arises whether one can observe isoscalar $E2$ strength relative to the much stronger isovector $E1$ strength, even if the $E2$ strength is concentrated in a sufficiently narrow region of excitation energies. As was pointed out in more detail in Sec. II, we might expect to observe a compact $E2$ resonance with the α capture reaction, since (i) for a self-conjugate nucleus like ^{24}Mg the isospin selection rule could strongly reduce the $E1$ strength, and (ii) very small contributions of $E2$ strength can be extracted from the angular correlation studies.

The unknown factor is, of course, whether the $E2$ resonance has enough α_0 decay width to be detected in the (γ, α_0) process. The results of the

present α -capture studies are shown in Fig. 10, where the amount of $E2$ strength integrated over 2 MeV wide intervals is given in percent of the $E2$ sum rule [Eq. (5)]. The data covering the region up to 14 MeV, taken from the literature,^{20,21} include bound levels (total $E2$ strength) and sharp resonances (all observed decay channels). A large amount of strength is concentrated in the first excited state ($\approx 20\%$). The rest of the known $E2$ strength is fairly evenly distributed over the entire region up to the expected center of the GQR which is marked by arrows in Fig. 10. There is some evidence of peaking around $E_x = 13$ MeV. Almost 50% of the $E2$ sum rule is accounted for below $63A^{-1/3}$ MeV. Since the α -capture reaction measures only the strength in the α_0 channel, the $E2$ strength found in the region above $E_x = 14$ MeV is only a lower limit and considerable strength may be associated with the decay into other channels. Thus, the isoscalar $E2$ strength spread out below $63A^{-1/3}$ is probably considerably greater than 50% of the sum rule.

These results can be compared with those obtained from inelastic scattering experiments. We find them to be inconsistent with a compact $E2$ resonance located just below the GDR as reported in (p, p') (Ref. 3) and ($^3\text{He}, ^3\text{He}'$) (Ref. 4) scattering for the neighboring nucleus ^{27}Al . We shall therefore restrict the discussion to α scattering, which is appropriate also for the following reasons.

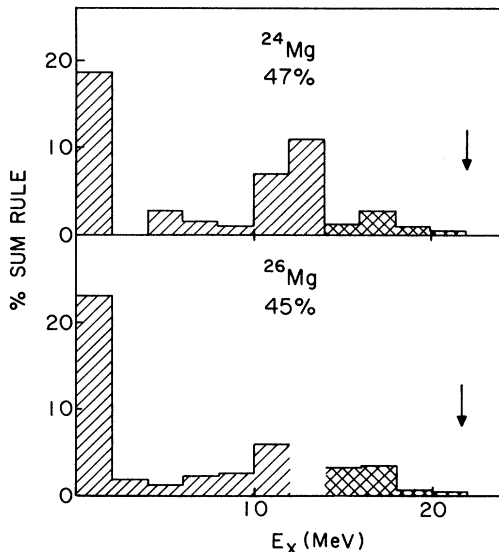


FIG. 10. The $E2$ strength integrated over 2 MeV intervals (in percentage of the energy-weighted sum rule) in the bound states (Ref. 10) and low lying resonances (Ref. 20) (shown by the dashed shading) and in the α_0 decay channel (cross-hatched), for both ^{24}Mg (top) and ^{26}Mg (bottom). The region around 12 MeV in ^{26}Mg has never been studied and is therefore left unshaded.

First, in p , ^3He , and electron scattering the GDR is also excited, while in α scattering only isoscalar modes will be observed. Second, only for inelastic α scattering⁵ has a systematic study of light nuclei been made. This study shows that below ^{40}Ca the GQR becomes progressively spread out over lower energies so that no compact resonance can be identified, in essential agreement with the present results. Additionally, a careful investigation of the distribution of $E2$ strength in ^{24}Mg has been performed by Singh and Yang²² using the reaction $^{24}\text{Mg}(\alpha, \alpha')$ at 70 MeV. Up to 17 MeV a rather uniform distribution was found in discrete levels which accounted for 40% of the sum rule. No strong peak at higher energies was observed which could be identified as a compact $E2$ giant resonance. The general picture emerging from these data is in agreement with our results in Fig. 10.

It has been argued that because of its complexity the α particle in capture is not a good probe for investigating giant resonances, since it can excite a giant resonance only through the compound nucleus. This seems to be true for the GDR where only a small fraction of the total strength ($<1\%$) is associated with the α_0 channel (see Sec. IV B), but appears to be doubtful in the case of the GQR. If it is assumed that the α -capture reaction excites only the compound nuclear (CN) part of the GQR, which in turn decays into various channels in a purely statistical way, then it is possible to derive the total absorption cross section for isoscalar $E2$ radiation $\sigma_{\text{tot}}^{\text{CN}}(E2)$ from the measured $\sigma(\gamma, \alpha_0)$ cross section using the theory of Hauser and Feshbach:

$$\sigma_{\text{tot}}^{\text{CN}}(E2) = \left(T_{\alpha_0} / \sum_i T_i \right)^{-1} \sigma(\gamma, \alpha_0), \quad (8)$$

where T_i denotes the transmission coefficient for

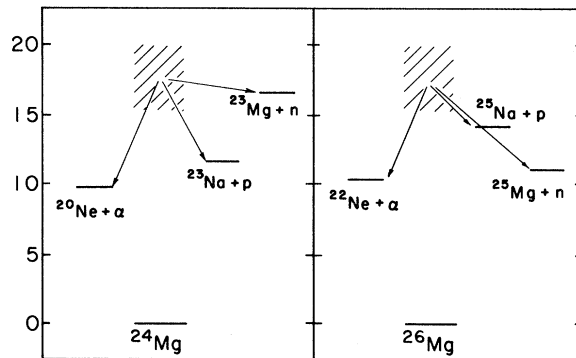


FIG. 11. Mass diagram showing the open channels for ^{24}Mg (left) and ^{26}Mg (right). In the decay of ^{26}Mg , neutron competition will be much more severe than in the decay of ^{24}Mg .

decay into one of the various p , n , or α channels shown in Fig. 11 for ^{24}Mg and ^{26}Mg .

We calculated the transmission coefficients T_i using the computer code ABACUS²³ and optical parameters as given in Ref. 24. The ratio $T_{\alpha_0}/\sum T_i$ thus obtained is shown in Fig. 12 as a function of energy for both ^{24}Mg and ^{26}Mg . Since the n channel for ^{26}Mg opens at 11 MeV (compared to 16.5 MeV for ^{24}Mg) the ratio $T_{\alpha_0}/\sum T_i$ is much smaller for ^{26}Mg throughout the energy region investigated. This leads to the interesting results for $\int \sigma_{\text{tot}}^{\text{CN}}(E2)/E^2 dE$ shown in Table II. For ^{24}Mg the assumption that $\sigma(\gamma, \alpha_0)$ is all compound gives an integrated strength that is somewhat in excess of the sum rule. However, since the sum rule depends on the choice of r_0 , a slightly higher but perhaps acceptable value of r_0 could produce agreement with the sum rule. Thus, there is no positive evidence for a noncompound component in $\sigma(\gamma, \alpha_0)$ in the $E2$ strength of ^{24}Mg . But in the case of ^{26}Mg , where almost the same strength is observed in the α_0 channel in the region 14–22 MeV, the assumption of a purely compound process leads to a total strength greatly in excess of the sum rule, $\approx 300\%$. Thus, we conclude that there must be an important noncompound component in $\sigma(\gamma, \alpha_0)$ in the $E2$ strength of ^{26}Mg .

In spherical nuclei such as ^{16}O and ^{40}Ca , the $E2$ strength has been calculated^{25,26} in terms of 1p-1h excitations of the $2\hbar\omega$ type. It is found that the isoscalar $E2$ strength is concentrated into a compact resonance around $63A^{-1/3}$ MeV. Since no such resonance is observed in ^{24}Mg or ^{26}Mg , we conclude that the present calculations are incomplete and should include more complex configurations such as 2p-2h, etc. It could be argued that the spread in $E2$ strength is due to the deformed nature

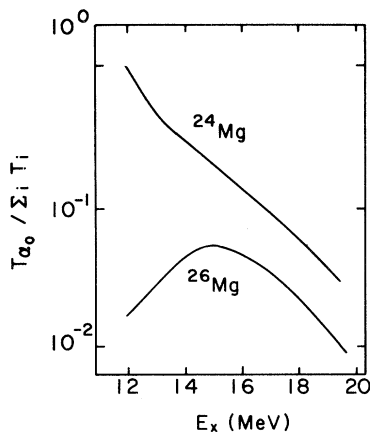


FIG. 12. The percentage of decays to the ground state α channel calculated from optical model parameters (Ref. 24).

of ^{24}Mg and ^{26}Mg . However, this spreading of the strength appears to be a universal characteristic of light nuclei below ^{40}Ca , including ^{16}O .⁵

B. Isospin mixing in the giant dipole resonance

The giant dipole resonances in ^{24}Mg and ^{26}Mg have been studied by various reactions such as (γ, n) ,¹⁵ (e, e') ,^{19,27} and (p, γ) .¹⁴ The integrated total strengths found in these reactions are compared with the present (α, γ) results in Table III. It can be seen that for both nuclei the strength associated with the α_0 decay is very small. This result is consistent with the assumption of a large direct component in a GDR, consisting basically of 1p-1h states which would inhibit the emission of α particles.

A second reason for a reduced α decay in ^{24}Mg may originate from the isospin selection rule. In a self-conjugate nucleus the GDR is $(J^\pi, T) = (1^-, 1)$, which can only decay into the α_0 channel if it is mixed into the $(J^\pi, T = 1^-, 0)$ states. In ^{26}Mg , however, the GDR can consist of two parts: one with $T_- = 1$ and the other with $T_+ = 2$. Both the (γ, n) ¹⁵ and the (e, e') ²⁶ results support the picture of a split GDR [see Fig. 7(c)], the T_- part covering the approximate range from 14.5 to 19.5 MeV and the T_+ part from 19.5 to 28.0 MeV. Only the lower part of the GDR can have an isospin-allowed α decay. Thus, the importance of the isospin selection rule can be tested by comparing the $^{20}\text{Ne}(\alpha, \gamma)$ and the $^{22}\text{Ne}(\alpha, \gamma)$ reactions.

It was found in the reaction $^{22}\text{Ne}(\alpha, \gamma)^{26}\text{Mg}$ (Table I) that the maximum intensity was indeed concentrated around 16 MeV with the average cross section being three times larger than that found in the same region for the reaction $^{20}\text{Ne}(\alpha, \gamma)^{24}\text{Mg}$. Since the neutron threshold in ^{26}Mg is much lower than in ^{24}Mg (Fig. 11), the number of open decay channels at about 16 MeV is approximately three times higher than at the same energy in ^{24}Mg . This will have the effect of lowering the relative importance of α_0 decay in ^{26}Mg compared to ^{24}Mg , so that the actual $E1$ strength in ^{26}Mg is probably considerably greater than three times that in ^{24}Mg .

The results obtained from the angular distribution studies and the cross-correlation analysis can be summarized as follows. For capture into ^{24}Mg it was found that (i) the average ratio of $E1/E2$ strengths was only 4:1; (ii) the shapes of the γ_1 angular distributions changed drastically with energy, yielding at the higher energies an average a_2 coefficient close to the one expected for decay through 3^- levels; (iii) no significant cross correlation between the γ_0 and the γ_1 yield curves was observed. On the other hand, for ^{26}Mg it was found that (i) the average ratio of $E1/E2$ strengths was

about 12/1; (ii) the shapes for both the γ_0 and the γ_1 angular distributions were almost constant, with average a_2 coefficients close to the ones expected for decay through 1^- levels; and (iii) a significant cross correlation was observed, indicating that some of the same 1^- levels were excited in both the $^{22}\text{Ne}(\alpha, \gamma_0)^{26}\text{Mg}$ and the $^{22}\text{Ne}(\alpha, \gamma_1)^{26}\text{Mg}$ reactions.

The above results suggest that isospin plays an important role in the decay of the GDR in ^{24}Mg in that it suppresses the decay of the 1^- levels. A comparison with the capture reaction $^{23}\text{Na}(p, \gamma)^{24}\text{Mg}^{14}$ in the region of the GDR also suggests that the isospin mixing might be small, as can be seen from the following arguments. The autocorrelation analysis¹⁴ of the γ_0 yield curve in the $^{23}\text{Na}(p, \gamma)$ reaction showed that about 50% of the observed radiation comes from the compound nucleus. From Table III we see, then, that the compound nuclear part of the GDR in ^{24}Mg has about a 1.6% branch for the ground-state protons. On the other hand, in the α -capture reaction which is believed to

proceed predominantly through the compound nuclear configuration, it was found (Table III) that the GDR has only about a 0.33% branch for ground-state α particles. Thus, the α_0 emission is reduced with respect to p_0 emission for the compound nuclear part of the GDR in ^{24}Mg , although the transmission coefficients for α_0 and p_0 are comparable. Hence the isospin may be rather pure. We recall that a totally different result was obtained in the investigation of the GDR in ^{28}Si ,⁶ where the α_0 emission from the compound nuclear part was found to be as great as the p_0 emission, which in turn suggested a large mixing of the isospin. It is evident that further information is needed to elucidate this question of the isospin mixing.

We would like to thank V. K. C. Cheng and J. R. Hall for assistance in taking the data; and Ken Williams, Jack Harris, and Ed Dillard for help in maintaining the equipment.

*Work supported in part by the National Science Foundation.

†Max Kade Postdoctoral Research Fellow, 1972–74.

‡Present address: Department of Physics, Ruhr Universität Bochum, Bochum, West Germany.

§Present address: Department of Physics, Rutgers University, New Brunswick, New Jersey 08903.

¹R. Pitthan and Th. Walcher, Phys. Lett. **36B**, 563 (1971); R. Pitthan, Z. Phys. **260**, 283 (1973).

²Y. Torizuka *et al.*, in *Proceedings of the International Conference on Photoneuclear Reactions and Applications, Asilomar, 1973*, edited by B. L. Berman (Lawrence Livermore Laboratory, Livermore, California, 1973), Vol. I, p. 675.

³M. B. Lewis and F. E. Bertrand, Nucl. Phys. **A196**, 337 (1972); F. E. Bertrand, E. E. Gross, D. J. Horen, D. C. Kocher, M. B. Lewis, and E. Newman, in ORNL Physics Division Annual Report, 1973 (unpublished).

⁴A. Moalem, W. Benenson, and G. M. Crawley, Phys. Rev. Lett. **31**, 482 (1973).

⁵L. L. Rutledge, Jr., and J. C. Hiebert, Phys. Rev. Lett. **32**, 551 (1974); D. Youngblood, J. M. Moss, C. M. Rozsa, J. D. Bronson, and A. D. Bacher, in Texas A&M University, Cyclotron Institute Progress Report, 1974 (unpublished), p. 1.

⁶L. Meyer-Schützmeister, Z. Vager, R. E. Segel, and P. P. Singh, Nucl. Phys. **A108**, 180 (1968).

⁷R. B. Watson, D. Branford, J. L. Black, and W. J. Caelli, Nucl. Phys. **A203**, 209 (1973); G. S. Foote, Ph.D. thesis, Australian National University, Canberra, 1974 (unpublished).

⁸K. A. Snover, E. G. Adelberger, and D. R. Brown, Phys. Rev. Lett. **32**, 1061 (1974).

⁹D. Branford, Particles and Nuclei **6**, 127 (1973).

¹⁰M. Suffert, W. Feldman, J. Mahieux, and S. S. Hanna, Nucl. Instrum. Methods **63**, 1 (1968).

¹¹F. Riess, in *Proceedings of the Decus Symposium, Decus, 1967* (Decus, Maynard, Mass., 1967), p. 159.

¹²M. Gell-Mann and V. Telegdi, Phys. Rev. **91**, 169 (1953).

¹³G. J. Highland and T. T. Thwaites, Nucl. Phys. **A109**, 163 (1968).

¹⁴R. C. Bearse, L. Meyer-Schützmeister, and R. E. Segel, Nucl. Phys. **A116**, 682 (1968).

¹⁵S. C. Fultz, R. A. Alvarez, B. L. Berman, M. A. Kelly, D. R. Lasher, T. W. Phillips, and J. McElhinney, Phys. Rev. **C 4**, 149 (1971).

¹⁶T. Ericson, Ann. Phys. (N.Y.) **23**, 390 (1963).

¹⁷P. J. Dallimore and I. Hall, Nucl. Phys. **88**, 193 (1966).

¹⁸A. Bohr and B. R. Mottelson, *Nuclear Structure* (Benjamin, New York, 1972), Vol. 2; T. Suzuki, Nucl. Phys. **A217**, 182 (1973).

¹⁹O. Titze, E. Spamer, and A. Goldmann, Phys. Lett. **24B**, 169 (1967); A. Goldmann, Z. Phys. **234**, 144 (1970).

²⁰P. M. Endt and C. Van der Leun, Nucl. Phys. **A214**, 1 (1973).

²¹E. W. Lees, A. Johnston, S. W. Brain, C. S. Curran, W. A. Gillespie, and R. P. Singhal, J. Phys. **A7**, 936 (1974); E. W. Lees *et al.*, in *Proceedings of the International Conference on Nuclear Physics, Munich, 1973*, edited by J. de Boer and H. J. Mang (North-Holland, Amsterdam/American Elsevier, New York, 1974), p. 621.

²²P. P. Singh and G. C. Yang, in *Proceedings of the International Conference on Nuclear Structure and Spectroscopy, Amsterdam, 1974*, edited by H. P. Blok and A. E. L. Dieperink (Scholar's Press, Amster-

dam, 1974), Vol. 1, p. 162.

²³E. H. Auerbach, Brookhaven National Laboratory Report No. 6562, 1962 (unpublished).

²⁴B. T. Lucas *et al.*, Phys. Rev. 144, 972 (1966); G. M. Crawley and G. T. Garvey, *ibid.* 167, 1070 (1968); E. Vogt, in *Advances in Nuclear Physics*, edited by M. Baranger and E. Vogt (Plenum, New York, 1968), Vol. 1.

²⁵S. Krewald, J. Birkholz, A. Faessler, and J. Speth,

in *Proceedings of the International Conference on Nuclear Structure and Spectroscopy, Amsterdam, 1974*, edited by H. P. Blok and A. E. L. Dieperink (see Ref. 22), Vol. 1, p. 31; and private communication.

²⁶G. F. Bertsch and S. F. Tsai, Michigan State University, unpublished.

²⁷O. Titze, A. Goldmann, and E. Spamer, Phys. Lett. 31B, 565 (1970).